SIMULATING THE OVERLOAD TEST FOR A 480 KN MAXIMUM HOOK LOAD WORKOVER RIG MAST

Aurelian IAMANDEI[1], Șerban Nicolae VASILESCU[2], Ioan POPA[3], Lavinia Silvia STANCIU[4], Răzvan George RÎPEANU[5]

Service rigs provide the possibility to carry out various operations at the well hole. Spatial metallic constructions intended to support the drilling crown-block, the crane-hook Assembly, the maneuvering cable, the stacking of the pipe steps, the placement of the floor man bridge are the masts. They must be subjected to an overload test which, according to the API 4F standard, is performed by computer simulation using software based on finite element analysis. This paper presents the results of such a simulation for a prototype mast of a service rig type IC 5, with a maximum hook load of 480 kN, followed by an experimental test made on the real prototype structure.

Keywords: workover rig, mast, overload test, finite element method.

1. Introduction

Within the installations used in the oil field, a large share has the service rigs. These transportable installations provide the possibility to perform various operations, such as inserting and removing the tubular material, changing the depth pumps, mounting and dismounting the christmas tree, repair and remediation works for wells such as: milling of cement plugs, washing of sand plugs, instrumentation, etc., pistoning and bailing operations, repairs of casings, various production tests [1, 2].

The masts that equip these service rigs consist of one or two sections with a latticed construction. In general, they are mounted folded on a trailer or truck, making a solid physical connection in order to obtain increased safety and the best

[1] Eng. SC IA Project SRL, PhD Student at Department of Mechanical Engineering from Petroleum-Gas University, Ploiești, Romania, e-mail: iamandei@ia-proiect.ro
[2] Prof. PhD. Eng., Department of Mechanical Engineering from Petroleum-Gas University, Ploiești, Romania, Romania, e-mail: vserban@upg-ploiesti.ro
[3] Assoc. Prof. Phd Eng., Department of Mechanical Engineering from Petroleum-Gas University, Ploiești, Romania, Romania, e-mail: apopnaoi@gmail.com
[4] Lecturer PhD Eng., Department of Mechanical Engineering from Petroleum-Gas University, Ploiești, Romania, Romania, e-mail: laviniastanciu@yahoo.com
[5] Prof. PhD. Eng., Department of Mechanical Engineering from Petroleum-Gas University, Ploiești, Romania, Romania, e-mail: rrapeanu@upg-ploiesti.ro

possible movement of the service rig at the location of the well. At that location the masts are telescoped to a quasi-vertical position [3, 4]. An inconvenience of this inclination is represented by the appearance of considerable additional stresses in the load-bearing structure of the mast. In order to reduce these stresses to some acceptable limits of the material of the mast bars, it is anchored at one or two levels with resistance anchors, their mounting being mandatory [3, 4, 5]. The anchors can be: internal (attached to the trailer or semi-trailer of the installation, two anchors at each level) and external (fixed to the ground, four anchors) [1]. In the case of anchored masts of service rigs, the influence of anchors shall also be taken into account when performing the design or verification calculation [5, 6].

These types of masts must undergo a very severe test called an overload test before they can be delivered to work at the borehole [3, 6]. The Romanian companies specialized in making such equipment adopted the API 4F standard developed by the American Petroleum Institute ("*Specification for Drilling and Well Servicing Structures*", Fifth Edition, June 2020 [5]). This standard no longer requires a physical experimental test but requires mast designers and manufacturers to perform a computer simulation of the overload test, using specialized software based on finite element analysis. In the following both computer simulation and experimental results will be presented.

The mast that is the subject of this paper is a prototype designed to equip a type IC 5 service rig (see Fig. 1) and supports a maximum hook load of 480 kN.

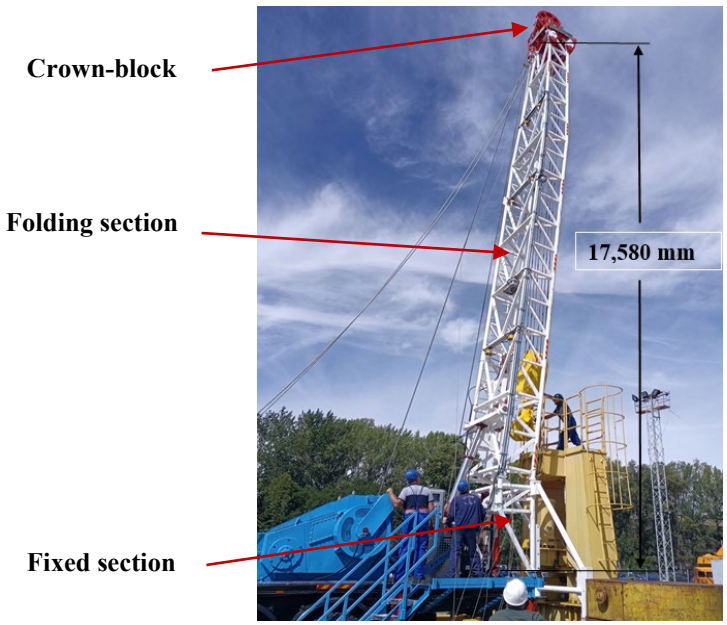

Fig. 1. The service rig with the mast prototype in working position, prepared for testing

2. General description of the mast

The mast consists mainly of two sections: a fixed section and a folding section. At the top of the folding section is the crown block, supported by it. The fixed section is connected by means of a chassis stabilizing structure. During transport to the place of operation, the folding section is placed horizontally on the truck. Prior to commissioning, this section is brought into the working position which is quasi-vertical (slightly inclined at an angle of 6.4° to the vertical), by means of a hydraulic cylinder. The total height from the ground in the working position is 17,580 mm, measured from the lower face of the crown-block. The fixed section-mast-crown block assembly is shown in Fig. 1, which presents the prototype of the mast.

In the operating position, the mast is anchored to the ground by means of four safety anchors (two at the front, two at the rear), and at the truck chassis by means of two resistance anchors of diameter Ø18, these being attached to the mast at the lower level of the crown of the window. The inclination of the resistance anchors in relation to the vertical axis is 31.4°.

The mast is a spatial construction, consisting mainly of circular, rectangular or square pipe type bars, having in the cross section on the area of the folding section the shape of the letter „U" (Fig. 2).

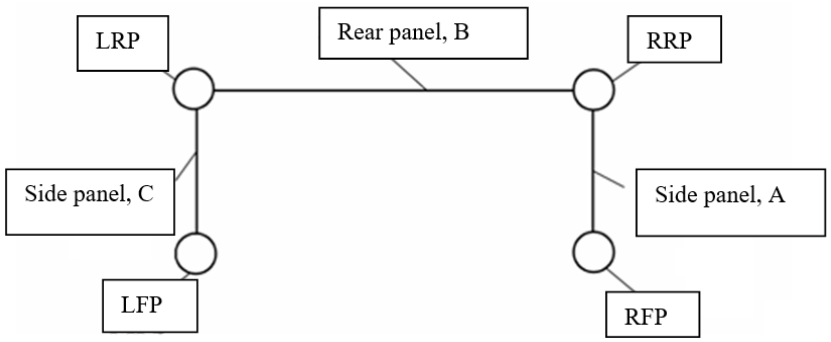

Fig. 2. The „U" shape of the cross-section of the folding section (LFP – left front pillar; RFP – right front pillar; LRP – left rear pillar; RRP – right rear pillar)

At the bottom, the mast has a joint between the folding section and the fixed one, which is located on the truck. In the quasi-vertical position, i.e. in the working position, the folding section is placed above the fixed one. The type of block is GF 40-4x22 type, the number of wires on the crane is 6, the diameter of the operating cable is Ø 22.

The fixed section is a structure [7] with a mass of 464.2 kg (including the stabilizing structure, 1069.67 kg) and a height of 1,822 mm measured from the axes of the mast and fork counterbraces, consisting mainly of circular pipe-type

bars welded together, ensuring rigid fixation to nodes. Its composition includes: Ø95x8, made of S355 J2 steel bars (EN 10210-1) - two of which are pillars, counterbraces of Ø95x8, made also of S355 J2 steel, stiffening bars with box cross-section of 60x60x4, S355 J2 steel, connecting bars with box cross-section of 60x60x4 made of S355 J2 steel, HEB 120 profile stiffeners made of S355 J2 steel, fork clamps for connection to counterbraces, pillars, and folding section, S355 J2 steel, and also plates and ribs made of S235 JR steel.

The folding section, generically referred to as the mast, is a structure with a total mass of approximately 1,500 kg and a height of 14,308 mm, with a „U”-shaped cross section. It consists mainly of circular, square, or rectangular pipe bars, welded together, which ensures rigid attachment to the nodes. The four pillars, noted in Fig. 2 with LFP, RFP, LRP, RRP, have the same Ø95x8 cross section and are made of S355 J2 steel (EN 10210-1). They wear the three sides panels of the mast - two lateral and a rear one, noted in Fig. 2 with A, B and C. This section includes various horizontal bars, diagonals (stiffeners) placed on side panels levels in the shape of the letter "V".

The crown block is a rigid structure, made of non-standard I profile beams 200 mm high, made of 10 mm thick plate, steel S355 J2, with the plates stiffened to heart by welding. The roller shafts are made of S355 J2 steel, with a solid circular section Ø108. The rollers, in number of 4 + 1, have a diameter of Ø560, and the wire rope that passes over them has a diameter of Ø22.

The main elements of the mast are made of S355J2 steel, SR EN 10025, which has the minimum offset yield strength $R_{p02} = 355\ MPa$, both tensile and compression, and the ultimate strength limit $R_m = (490 \dots 630)\ MPa$. For this material, the standard API 4F Fifth Edition refers in Chapter 8, Subchapter 8.1, to ANSI/AISC 360-16 standard (regarding the "Allowable Strength Design code"). Axial, tensile, or compressive stresses are defined in the standard as the principal stresses occurring in such a latticed structure, and those arising from bending moments as secondary stresses. Allowable strength of the material, as specified by ANSI/AISC 360-16, is defined as the ratio of:

$$\sigma_a = \frac{R_n}{\Omega} \tag{1}$$

where R_n is the nominal strength and Ω a safety factor. In Annex B of the API 4F standard, in subchapter B.8.1.1, it is recommended to use a safety factor of 0.66 (which is the inverse of the safety factor, Ω), in accordance with AISC 335-89 (relation F3-1, page 5-48). Thus, the allowable strength that is further considered in this analysis is:

$$\sigma_a = 0.66 \cdot R_{p02} = 234\ MPa \tag{2}$$

In this situation, the strength condition is:

$$|\sigma|_{max} \leq \sigma_a \tag{3}$$

3. Computer simulation of mast behaviour during the overload test

Computer simulation using FEA is the appropriate way to realize structural analyses [7-15]. In the case of this mast prototype, the loads are: the overload force Q_p = 560 kN = 1.167 Q_{max}, where Q_{max} = 480 kN is the maximum hook load, and 1.167 is the overload factor taken into account for the expected working conditions; the weight of the hoisting system, Q_m = 30 kN; the dead weight of the mast assembly. The dead weight of the mast is determined automatically by the software Ansys [12], entering as input data the density of the steel, ρ = 7,850 kg/m^3, the dimensions of the cross-sections of the bars and the coordinates of the nodes, with the help of which the length of each element is determined. The test load and the weight of the hoisting system are applied statically at the crown block level (conceptual model in Fig. 3). In this case, the force in the wire rope is considered constant along its entire length. According to [5, 9, 11], the mast is analyzed assuming that it works together only with the two resistance anchors, without tying by ground with safety anchors.

The resulted model included [7]: 170 points - including here the points that serve to orient some cross-sections or to orient the fast line and the dead line of the wire rope, 299 lines, 744 nodes, six types of ground connections (spatial roller supports) – two for connecting the anchors and four for connecting the fixed section to the folding one, and 299 finite elements (each line was considered a finite element) - 295 elements BEAM 189 type, two elements LINK 10 type for the strength anchors and two elements LINK 8 type for the two counterbraces from the fixed section.

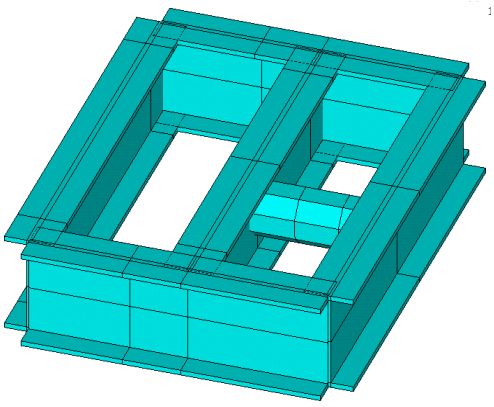

Fig. 3. Conceptual model for the main frame of the crown block

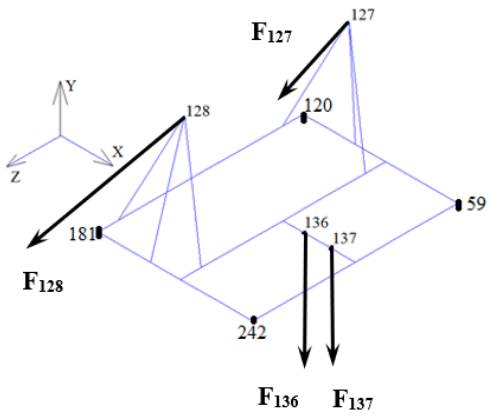

Fig. 4. Crown block scheme showing the points for introducing the forces

In Fig. 4 it is shown the scheme of the crown block on which are specified the points where the forces corresponding to the overload test were introduced. Point 127 is located on the wheel axle on which the dead line of the wire rope is

wrapped up and item 128 on the wheel axle on which the fast line of the wire rope is wrapped up. The dead line is in a plane parallel to the XY plane and makes an angle $\beta \approx 9.8°$ with the vertical. The fast line is also in a plane parallel to the XY plane and makes an angle $\gamma \approx 13.9°$ with the vertical.

Considering that the crane of the traveling block has three rollers, a force of 98,333 N (590:6 = 98.333 kN) arises in the wire rope so that the total load of 590 kN (560 kN – the overload force and 30 kN – the weight of the hoisting system) is introduced in the points at the level of the crown block as follows:

-in the point 127,

- along the general axis X, in the opposite direction, a force $F_{127,X} = -98{,}333 \cdot \sin\beta = -16{,}737$ N;
- along the general axis Y, in the opposite direction, a force $F_{127,Y} = -98{,}333 \cdot \cos\beta - 98{,}333 = -195{,}231$ N;

-in the point 128,

- along the general axis X, in the opposite direction, a force $F_{128,X} = -98{,}333 \cdot \sin\gamma = -23{,}622$ N;
- along the general axis Y, in the opposite direction, a force $F_{128,Y} = -98{,}333 \cdot \cos\gamma - 98{,}333 = -193{,}786$ N;
- in the points 136 and 137, along the general axis Y, in the opposite direction, two forces $F_{136,Y} = F_{137,Y} = -98{,}333 \cdot 2 = -196{,}666$ N.

The calculation of the mast is performed using Ansys, considering only the two resistance anchors with a diameter of 18 mm. After running the software, the displacements of all the nodes of the structure are obtained. Its deformed shape is shown in Fig. 5. It is noticed that the mast moves, following the application of the test load, towards the positive direction of the general axis X and has a maximum total displacement of 49.8 mm. This occurs, as it is expected, at the crown block level.

In Fig. 6 it is shown the deformed shape of the crown block (where there are also the biggest displacements of the mast structure). It is noticed that the block has the predominant displacement in the direction of the X axis (towards the wellbore), but it also has a clockwise rotation, which is explained by the fact that the fast line is less inclined to the vertical and, thus, has a horizontal component force bigger than one of the dead line. This rotation results in a general torsion of the mast. In Table 1 are presented the three-axis displacements of the nodes of the corners of the crown block frame, where "USUM" is the total displacement.

Table 1

Displacements at the crown block level, *mm*

NODE	UX	UY	UZ	USUM
59	47.241	-15.314	4.0799	49.828
120	47.222	-11.612	1.3268	48.647
181	43.545	-11.255	1.3110	44.996
242	43.565	-14.544	4.0607	46.108

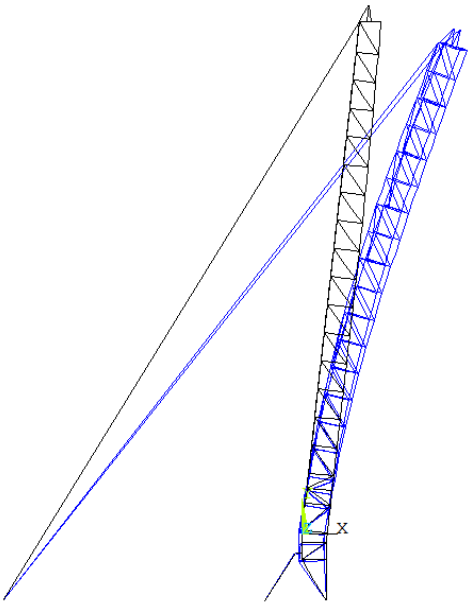

Fig. 5. The deformed shape of the mast during the overload test

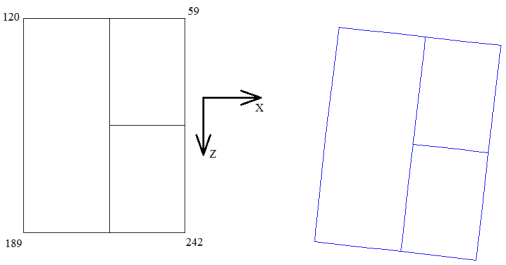

Fig. 6. Displacements at the crown block level

In Fig. 7 it is shown the general map of the stresses σ_x. The highest stresses, in absolute value, are recorded in the connection area between the fixed section and the folding section and have the maximum value $|\sigma_x| = 217$ MPa. The maximum stresses are recorded on the pillars and here the stress produced by the axial force predominate. In the two strength anchors (which can be seen in Fig. 7) the stresses that occur are: $\sigma_1 = 166$ MPa, respectively $\sigma_2 = 147$ MPa. The two values are different due to the different vertical inclination of the dead line and the fast line of the wire rope.

An area with a special behaviour is represented by the transition from the prismatic to the truncated pyramidal shape (Fig. 8). In this area, faces A and C become flared, which leads to a pronounced bending of the bars on face B.

In Fig. 9 it is shown the stress map for the elements that make up the folding section of the mast. The minimum stresses are at the base of a pillar, in the connection area with the fixed section. The maximum stresses appear in a horizontal beam located in the transition zone from the prismatic to the truncated pyramidal part. The maximum stress level in this area is about 196 MPa. Fig. 10 shows the stress map in the fixed section. The minimum stresses, of -217 MPa, appear in the connection area between the fixed and folding section. The maximum stresses, of 212 MPa, occur in the connection area between a horizontal beam and the pillar, in the vicinity of a counterbrace.

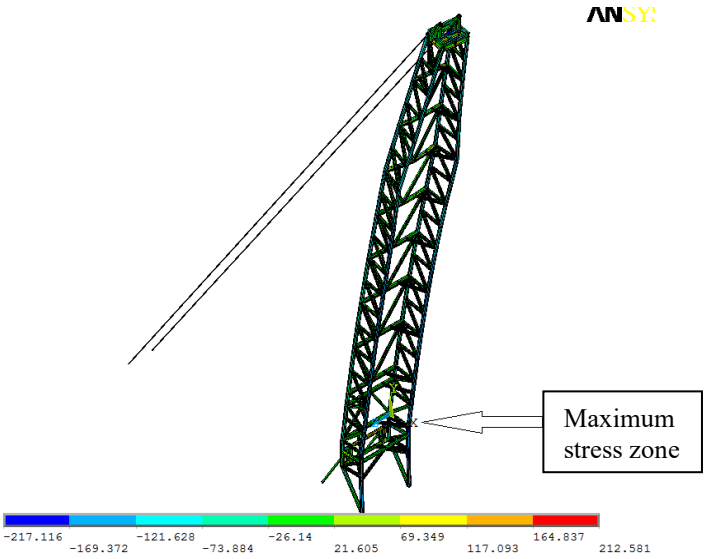

Fig. 7. Normal stress map for the assembly

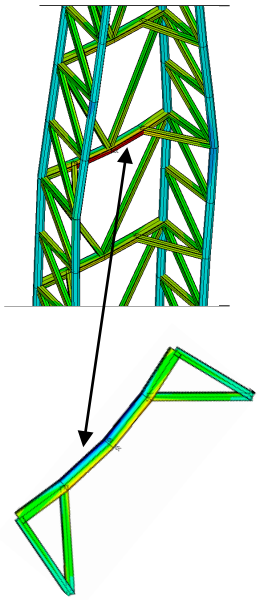

Fig. 8. Beam deformation in the transition zone from prismatic shape to truncated pyramidal one

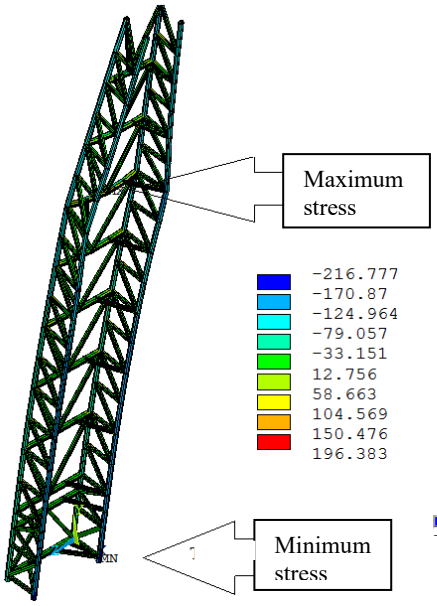

Fig. 9. Stress map in the folding section components

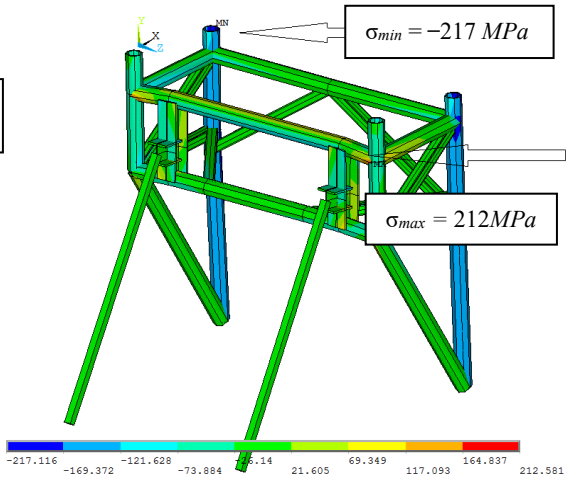

Fig. 10. Stress map in the fixed section components

6. Experimental results for the mast prototype

In order to validate the theoretical results obtained using FEA in the case of the overload test, an experimental work has been performed for the 480 kN maximum hook load service rig mast (Fig.1). In accordance with API 4F Fifth Edition, subchapter 11.8.1, the overload test (proof test) „is not a requirement" of the standard, while the computer simulation usig FEA is. But if specified by the purchaser, this severe test shall be made in accordance with Annex A.2 of the standard, to „a load agreed by the purchaser and manufacturer", and „the equipment shall be visually examined in accordance with 11.4.2 subchapter", which reffers only to critical welds that need to be 100% visually examined.

From the analysis carried out following the computer simulation of the overload test, it was found necessary to place 18 strain gauges in the most stressed zones, i.e. at the base of the four pillars, on the horizontal beam connecting the prismatic zone to the truncated pyramid one, and at the upper part of the pillars, near the crown block.

Fig. 11. Data aquisition system

Fig. 12. Strain gauge placed at the bottom of a pillar

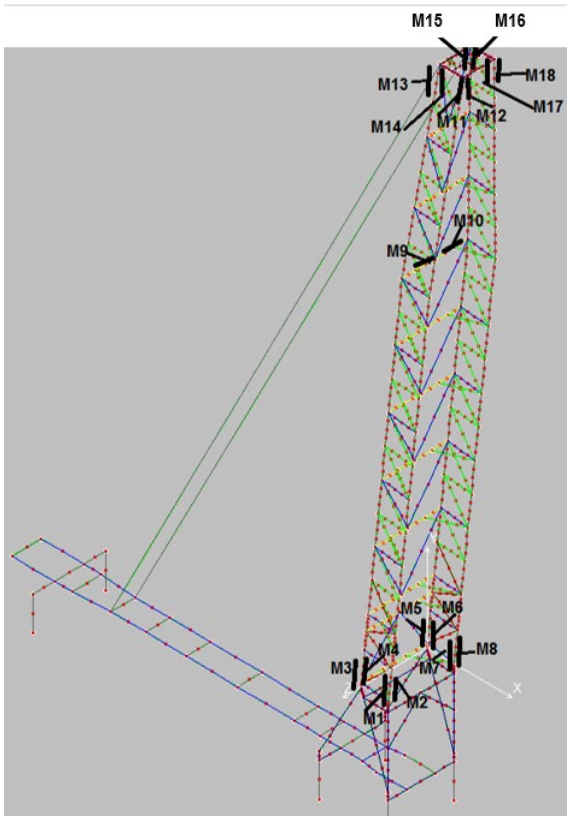

Fig. 13. The 18 strain gauges placed in points of the mast assembly

The experimental work has been completed by the authors using a HBM aquisition system loaded with a specialysed soft, „Catman®Easy" [13] (Fig. 11). The data aquisition system was connected with 18 strain gauges of 350 Ω (Fig. 12), and the measurements have been carried out providing the overload force of 560 kN (56 tf). The way in which the strain gauges were placed at certain points on the mast is shown in Fig. 13. As it can be noticed, the M1...M8 strain gauges are located near the junction between the four pillars from the folding section and the corresponding beams from the fixed section. The M9 and M10 strain gauges are located on the horizontal beam connecting the prismatic zone to the truncated pyramid one, and M11...M18 at the top of the four pillars, near the connection with the crown block.

All necessary measurements were performed during the overload test and were divided into three significant steps: 1. lifting the mast from the horizontal position to the working position; 2. overload test; 3. lowering the mast to the horizontal position. The variation of the overload force, in tf, as a function of time, in minutes, is shown in Fig. 14, from which it can be seen that the lifting process of the mast lasted about 20 minutes (including the preparation of the traction device), the overload test about 50 minutes (before that, with steps of 5 minutes each at 160 kN, 260 kN, 360 kN and 460 kN; the overload force of 560 kN was maintained for about 40 minutes) and for the lowering process, about 20 minutes. It can be also observed that the loading process was carried out at a speed of approximately 5 kN/min. The unloading process was slightly faster than the loading process, the unloading speed being about 20 kN/min.

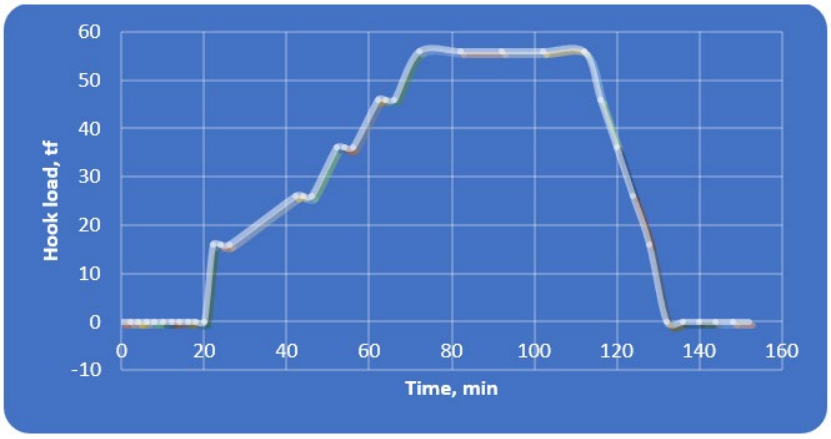

Fig. 14. The variation of the hook load against time during the experimental test

The most important of the many values of the strains recorded during the test are presented in Tables 2 and 3 below. Converting the strains into stresses by using the Hooke's law, the values presented in Tables 4 and 5 have been obtained.

Table 2

Strain values obtained with strain gauges M1...M10

Force, tf	M1, M2		M3, M4		M5, M6		M7, M8		M9, M10	
	ε_1, µm/m	ε_2, µm/m	ε_3, µm/m	ε_4, µm/m	ε_5, µm/m	ε_6, µm/m	ε_7, µm/m	ε_8, µm/m	ε_9, µm/m	ε_{10}, µm/m
16	-261	-263	-112	-116	-112	-115	-268	-275	243	244
26	-423	-427	-183	-188	-182	-186	-434	-446	393	396
36	-583	-587	-251	-259	-251	-256	-597	-614	541	544
46	-744	-749	-321	-331	-320	-326	-762	-783	691	695
56	-903	-911	-390	-402	-389	-396	-926	-951	839	844

Table 3

Strain values obtained with strain gauges M11...M18

Force, tf	M11, M12		M13, M14		M15, M16		M17, M18	
	ε_{11}, µm/m	ε_{12}, µm/m	ε_{13}, µm/m	ε_{14}, µm/m	ε_{15}, µm/m	ε_{16}, µm/m	ε_{17}, µm/m	ε_{18}, µm/m
16	-84	-94	-236	-263	-238	-265	-182	-204
26	-136	-152	-383	-427	-385	-430	-296	-331
36	-188	-210	-527	-587	-530	-592	-407	-456
46	-239	-268	-672	-750	-676	-755	-519	-581
56	-291	-325	-817	-911	-822	-917	-631	-707

Table 4

Stress values obtained with strains measured in strain gauges M1...M9

Force, tf	M1, M2		M3, M4		M5, M6		M7, M8, M9		
	σ_1, MPa	σ_2, MPa	σ_3, MPa	σ_4, MPa	σ_5, MPa	σ_6, MPa	σ_7, MPa	σ_8, MPa	σ_9, MPa
16	-54.85	-55.29	-23.66	-24.39	-23.63	-24.06	-56.19	-57.75	50.95
26	-88.89	-89.61	-38.35	-39.53	-38.29	-38.99	-91.07	-93.60	82.58
36	-122.36	-123.34	-52.79	-54.42	-52.70	-53.67	-125.36	-128.84	113.67
46	-156.12	-157.38	-67.35	-69.44	-67.25	-68.48	-159.96	-164.39	145.04
56	-189.70	-191.23	-81.84	-84.37	-81.71	-83.21	-194.36	-199.75	176.23

Table 5

Stress values obtained with strains measured in strain gauges M10...M18

Force, tf	M10, M11, M12			M13, M14		M15, M16		M17, M18	
	σ_{10}, MPa	σ_{11}, MPa	σ_{12}, MPa	σ_{13}, MPa	σ_{14}, MPa	σ_{15}, MPa	σ_{16}, MPa	σ_{17}, MPa	σ_{18}, MPa
16	51.24	-17.65	-19.74	-49.60	-55.29	-49.88	-55.67	-38.30	-42.89
26	83.05	-28.60	-32.00	-80.38	-89.61	-80.85	-90.23	-62.08	-69.52
36	114.31	-39.37	-44.04	-110.64	-123.34	-111.28	-124.20	-85.45	-95.69
46	145.86	-50.24	-56.19	-141.17	-157.38	-142.00	-158.48	-109.03	-122.09
56	177.23	-61.04	-68.28	-171.53	-191.17	-172.53	-192.56	-132.48	-148.35

Using all the measured values over the entire time interval during which the test was conducted (raising the mast from the horizontal position to the working position-overload test-lowering the mast to the horizontal position), the stress values versus time were graphically represented for each measurement point. The highest stress values, corresponding to points where strain gauges M1, M2, M7, M8, M9, M10, M15, M16 were placed are presented in Fig. 15...Fig. 18, where the stresses are specified with the number of each strain gauge.

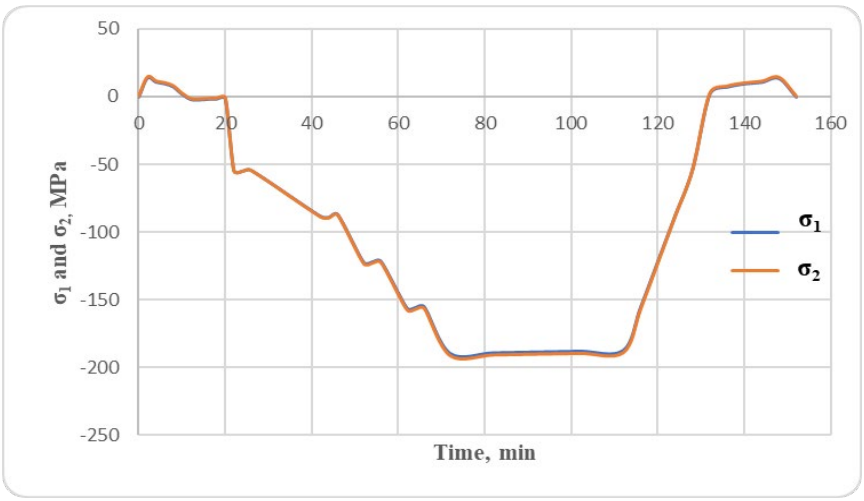

Fig. 15. Stress versus time in the points where M1 and M2 were placed

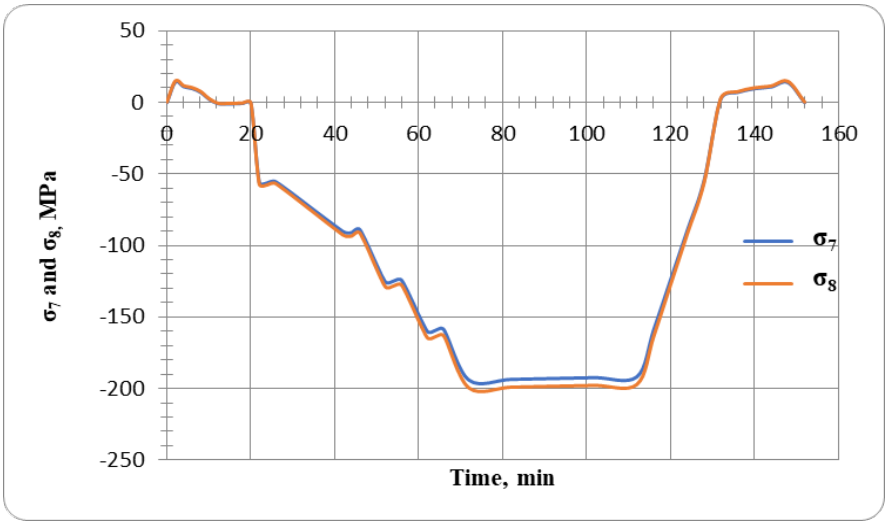

Fig. 16. Stress versus time in the points where M7 and M8 were placed

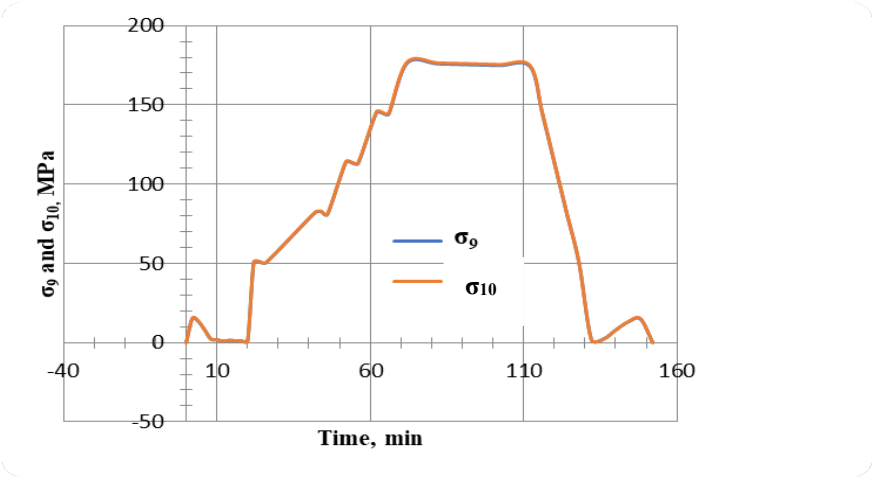

Fig. 17. Stress versus time in the points where M9 and M10 were placed

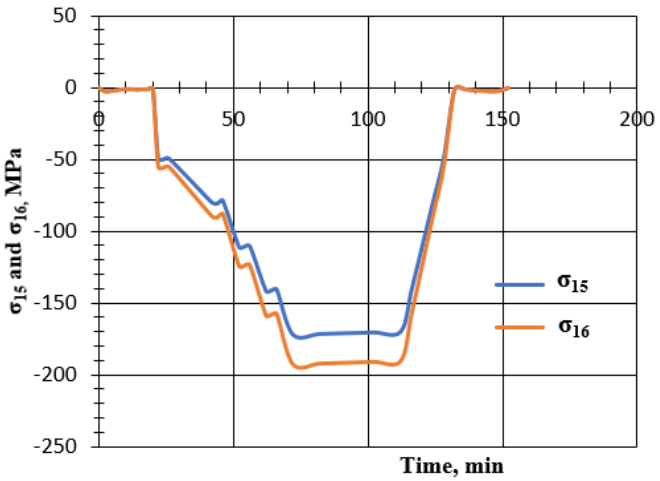

Fig. 18. Stress versus time in the points where M15 and M16 were placed

Analyzing all the data obtained for stress whose most important values have been presented in Tables 4 and 5 and the graphs shown in Fig. 15...Fig. 18, the following aspects can be highlighted:

- the values of the axial stresses, measured on the strain gauges placed in pairs (M1-M2, ..., M17-18) on the mast components, are approximately equal, which is to be expected, since the four pillars are stressed mainly in tension or compression and less in bending; the small differences that occur between the values indicated by the paired strain gauges are below 10% and come from the bending that occurs at the lower part of the uprights;

- the stress values have linear variations in time and respect the ranges of 160 kN, 260 kN, 360 kN, 460 kN and 560 kN forces that made up the overload experimental test;
- during the raising-lowering process of the folding section, the strain values, respectively the stress values recorded small oscillations produced by the dynamic effects (shocks) occurring both at the moment of starting the raising and during the lowering the mast on the fixed section; these effects had small values, below 40 MPa, and were quickly damped;
- the highest stress values were recorded at measurement points M1-M2 and M7-M8, which are points located at the inferior part of the pillars; the stress values occurring at these points were about 200 MPa (199.75 MPa), being below the value of the allowable strength of the material of 234 MPa [5, 14];
- the highest stress values for the points located at the top of the rear pillars, near the crown block, were reported at the measuring points M13-M14 and M15-M16; the stress values occurring at these points were about 193 MPa;
- when the mast returned to the horizontal position, i.e. after cancelling the overload force and the effects of dead weight, there was no deformation of any section of the mast, which shows that the whole overload test was carried out in the elastic domain.

7. Conclusions

1. The computer simulation using FEA of the overload test for the 480 kN (48 tf) maximum hook load mast was performed in accordance with the provisions of the API 4F Fifth Edition, 2020. For this purpose, it was used the specialized finite element analysis software Ansys 10.0.
2. The overload test is the most severe load and measures the strength of the mast. Based on the software calculation, it turned out that the mast has a good behaviour, the highest stresses, in absolute value, being seen in the connection area between the fixed section and the mast, being 217 MPa, under the steel allowable stress value of 234 MPa.
3. The transition zone from the prismatic to the truncated pyramidal shape has a special behaviour: here the sides panels A and C become flared, this phenomenon leading to a pronounced bending of the beams on the face B (see Fig. 2 and Fig. 8). The maximum stress in this area is approximately 196 MPa.
4. At the level of the crown block, the most stressed element is the central beam on which the axis of the block rests. The maximum stress level is 196 MPa, and the maximum displacement that is recorded at its level is about 50 mm.
5. The calculation of the mast was performed considering only the strength anchors, in the absence of safety anchors. In the two strength anchors (which can be seen in Figs. 1, 5 and 7) the stresses that appear are: σ_1 = 166 MPa,

respectively σ_2 = 147 MPa. The two values are different due to the different vertical inclination of the dead line and fast line of the wire rope.

6. The loads for the overload test were: Q_p = 560 kN = 1.167 Q_{max}, where Q_{max} = 480 kN is the maximum load on the hook, and 1.167 is the overload factor considered for the expected working conditions, the weight of the hoisting system, Q_m = 30 kN, as well as the dead weight of the mast assembly. The computer simulation showed that the prototype mast of 480 kN maximum hook load that is part of the transportable service rig at the wells has a good behaviour at this type of load, emphasizing that this is true in the case of an overload factor of 1.167.
7. The computer simulation of the overload test was followed by an experimental one. This test validated the results obtained using Ansys software. There were placed 18 strain gauges in the most stressed zones, i.e. at the base of the four pillars, on the horizontal beam connecting the prismatic zone to the truncated pyramid one, and at the upper part of the pillars, near the crown block, and a HBM data aquisition system loaded with a specialysed soft, „Catman®Easy", was used. The total testing duration was about 135 minutes (with steps of 5 minutes each at 160 kN, 260 kN, 360 kN and 460 kN; the overload force of 560 kN was maintained for about 40 minutes).
8. The highest stress values were recorded during the experimental test at measurement points located at the inferior part of the pillars; the stress values occurring here were about 200 MPa (199.75 MPa), being below the value of the allowable strength of the material of 234 MPa. The stress value obtained in the same points, using Ansys software, was 217 MPa. The two obtained values are very close.
9. Another important zone for the present analysis was the one that makes the transition from the prismatic shape to the truncated pyramid one of the folding section. During the experimental test there was recorded a stress value of 193 MPa, which is very close to the one obtained using computer simulation, of 196 MPa.
10. When the mast returned to the horizontal position, i.e. after cancelling the overload force and the effects of dead weight, it was found that there was no deformation of any section of the mast, which shows that the whole overload test was carried out in the elastic domain. At the same time, no welded zones were affected.
11. The stress and strain values obtained from the experimental testing were very close to those obtained from the computer simulation, which means that the authors of this paper correctly designed the components of the 480 kN maximum hook force mast prototype and performed a faithful simulation of the overload test. Thus, the IC 5 service rig mast can be judged to work safely at the wellbore.

R E F E R E N C E S

[1]. *A. Bublic, V. Cristea, I. Hirsch, N. Peligrad, Gh. Silion*, Utilaj petrolier pentru foraj și extracție (Oilfield equipment for drilling and extraction), Editura Tehnică, București, 1968.

[2] *** Confind Câmpina Company, http://www.confind.ro/instalatii_interventie_sonde.html, accessed March 2022.

[3] *I. Popa, L. S. Stanciu*, „Overload Test Behaviour Simulation Using FEA for a 320 kN Service Rig Mast”, Buletinul Universităţii Petrol-Gaze din Ploieşti, **Vol. LXVIII,** No. 4/2016, Seria Tehnică, pp. 73-78.

[4] *L. S. Stanciu, I. Popa*, „Study of the behaviour of a transportable mast of 500 kN maximum hook load during the free vibrations”, Buletinul Universităţii Petrol-Gaze din Ploieşti**,** Technical Series, **Vol. LXVII,** No.3/2015, pp. 45-52.

[5] *** American Petroleum Institute API, API 4F Standard, „Specification for Drilling and Well Servicing Structures”, Fifth Edition, June 2020.

[6] *L. S. Stanciu, I. Popa*, „Optimization Design of a 500 kN Workover Rig Mast after Computer Simulated Overload Test”**,** Applied Mechanics and Materials**, Vols. 809-810** (2015), pp. 932-937.

[7] *A. Iamandei, Ș. N. Vasilescu, I. Popa, L. S. Stanciu, R. G. Rîpeanu,* „Analysis of the behaviour of a 480 kN maximum hook load workover rig mast in the case of wind stress”, U.P.B., Sci. Bull., Series D, **Vol. 83**, Iss. 4, 2021, pp. 183-194.

[8] *I. Popa, L. S. Stanciu*, „Research Regarding Drilling Masts Reliability under the Combined Action of the Wind and the Hook Load”, Tribology in Industry, **vol. 37**, No. 1 (2015), pp. 29-33.

[9] *I. Popa, L. S. Stanciu*, „Stress and displacements analysis for drilling mast elements made of rectangular pipe: the overload test case”, Key Engineering Materials, **Vol. 601** (2014), pp. 120-123.

[10] *Al. Pupăzescu, I. Popa, L. S. Stanciu*, „The Evaluation of the Stress and Strain Condition for the Mast MU 320 Made out of U and I Profile Beams”, Buletinul Universităţii Petrol-Gaze din Ploieşti, Technical Series, **Vol. LX**, Nr. 3A/2008, pp. 223-228.

[11] *I. Popa, L. S. Stanciu*, „The study of The Static Behaviour of a Transportable Mast in Case of the Overload Test”, Buletinul Universităţii Petrol-Gaze din Ploieşti, Technical Series, **Vol. LX,** Nr. 3A/2008, pp. 217-222.

[12] *** Ansys Release 10.0 Software, Ansys Guide, 2006.

[13] *** Catman®Easy software, http://spectromas.ro/wp-content/uploads/2018/01/Fisa-tehnica-Catman.pdf, accessed August 2022.

[14] *** ANSI/AISC 360-16, Specification for Structural Steel Buildings, July 2016.